References

AGRAWAL, V. K. & TRIGUNAYAT, G. C. (1969). *Acta Cryst.* A**25**, 401-407.
AGRAWAL, V. K. & TRIGUNAYAT, G. C. (1970). *Acta Cryst.* A**26**, 426-429.
ALEXANDER, E., KALMAN, Z. H., MARDIX, S. & STEINBERGER, I. T. (1970). *Philos. Mag.* **21**, 1237-1246.
BOOTSMA, G. A., KNIPPENBERG, W. F. & VERSPUI, G. (1971). *J. Cryst. Growth*, **8**, 341-353.
CHAND, M. & TRIGUNAYAT, G. C. (1975). *J. Cryst. Growth*, **30**, 61-65.
CHAND, M. & TRIGUNAYAT, G. C. (1977). *J. Cryst. Growth*, **39**, 299-304.
CHAUDHARY, S. K. & TRIGUNAYAT, G. C. (1982). *J. Cryst. Growth*, **57**, 558-562.
CHAUDHARY, S. K. & TRIGUNAYAT, G. C. (1983). *J. Cryst. Growth*, **62**, 398-400.
CHAUDHARY, S. K. & TRIGUNAYAT, G. C. (1986). *J. Cryst. Growth*, **73**, 543-545.
HANOKA, J. I. & VAND, V. (1968). *J. Appl. Phys.* **39**, 5288-5297.
HAYASHI, A. (1960). *J. Mineral. Soc. Jpn*, **4**, 363-371.
JAIN, P. C. & TRIGUNAYAT, G. C. (1980). *J. Cryst. Growth*, **48**, 107-113.
KNIPPENBERG, W. F. (1963). *Philips Res. Rep.* **18**, 161-274.
KOZIELSKI, M. J. (1976). *Bull. Acad. Pol. Sci. Ser. Sci. Chim.* **24**(5), 367-375.
LAL, G. & TRIGUNAYAT, G. C. (1971). *J. Cryst. Growth*, **11**, 177-181.
LAL, G. & TRIGUNAYAT, G. C. (1974). *J. Solid State Chem.* **9**, 132-138.
LAWSON, W. D. & NIELSON, S. (1958). *Preparation of Single Crystals*. London: Butterworths.
LUNDQVIST, D. (1948). *Acta Chem. Scand.* **2**, 177-191.
MARDIX, S. & STEINBERGER, I. T. (1970). *J. Appl. Phys.* **41**, 5339-5341.
MEHROTRA, K. (1978). *J. Cryst. Growth*, **44**, 45-49.
MINAGAWA, T. (1975). *Acta Cryst.* A**31**, 823-824.
MITCHELL, R. S. (1962). *Z. Kristallogr.* **117**, 309-318.
PRASAD, R. & SRIVASTAVA, O. N. (1974). *Acta Cryst.* B**30**, 1748-1750.
SHARMA, G. L. (1980). PhD Thesis, IIT, Delhi.
TRIGUNAYAT, G. C. (1971). *Phys. Status Solidi A*, **4**, 281-303.
TRIGUNAYAT, G. C. & VERMA, A. R. (1976). *Physics and Chemistry of Materials with Layered Structures*, Vol. 2, edited by F. LEVY. Dordrecht: D. Reidel.
WAHAB, M. A. & TRIGUNAYAT, G. C. (1981). *Solid State Commun.* **36**, 885-889.

Acta Cryst. (1987). B**43**, 230-238

Atom Distributions in Tau-Carbide Phases: Fe and Cr Distributions in $(Cr_{23-x}Fe_x)C_6$ with $x = 0$, $0{\cdot}7_4$, $1{\cdot}7_0$, $4{\cdot}1_3$ and $7{\cdot}3_6$*

BY H. L. YAKEL

Metals and Ceramics Division, Oak Ridge National Laboratory, PO Box X, Oak Ridge, Tennessee 37831, *USA*

(*Received* 27 *May* 1986; *accepted* 2 *January* 1987)

Abstract

Mo $K\alpha$ Bragg diffraction data collected from single crystals of the title phases were used in least-squares refinements of structural models that (for $x \neq 0$) included *a priori* distribution parameters for iron on three of the four metal-atom sites of the known $M_{23}C_6$ τ-carbide structure. Conventional data for the crystal with $x = 0{\cdot}7_4$ were supplemented by synchrotron-radiation (SR) diffraction data collected at energies near Cr K and Fe K absorption edges. Results show that distribution parameters whose differences from chemical-average values have statistical and physical significance can be derived from extensive, precise conventional diffraction data. They demonstrate that iron atoms preferentially substitute for chromium at sites not bonded to carbon atoms; when 30-35% of the sites that are bonded to carbon are occupied by iron, the τ solid solution becomes thermodynamically unstable relative to other phases. Calculations with the SR data sets collected near the Cr K-edge energy suggest a $(\sin\theta)/\lambda$ dependence of the real part of the dispersion correction to the atomic scattering factor for chromium as well as significant departures from the theoretical free-atom calculations for these corrections at $(\sin\theta)/\lambda = 0$.

Introduction

Tau- (τ-) carbide phases formed during heat treatment of many iron- and chromium-based alloys that contain carbon can adversely affect the mechanical properties of such technologically important materials as ferritic and austenitic stainless steels (Shaw & Quarrell, 1957; Lai & Meshkat, 1978). Possible control of such effects will follow only from detailed studies of various properties of τ-carbide phases, among which crystal structure must be deemed especially relevant.

Basic features of the crystal structure of all τ carbides were first determined by Westgren (1933). Working with a phase whose composition was thought to be Cr_4C, Westgren found that X-ray diffraction and density measurements were more consistent with the formula $Cr_{23}C_6$. The carbide crystallized in the cubic system with a face-centered lattice ($a_0 \simeq 10{\cdot}66$ Å) in which 92 metal atoms were located at the 4(a), 8(c), 32(f) and 48(h) symmetry sites of space group $Fm\bar{3}m$ (see Fig. 1). Carbon atoms were most reasonably placed on 24(e) sites (E), a result later confirmed by neutron diffraction studies (Meinhardt & Krisement, 1962). Though described

* Research sponsored by the Division of Materials Sciences, US Department of Energy under contract No. DE-AC05-840R21400 with the Martin Marietta Energy Systems, Inc.

0108-7681/87/030230-09$01.50

differently by Westgren and others, the τ-carbide structure may be viewed as a network of edge-sharing, non-interpenetrating Friauf polyhedra (Samson, 1964). Each full Friauf polyhedron consists of 12 metal atoms on 48(h) sites (H) forming a tetrahedron truncated at each corner and 4 atoms on 32(f) sites (F) capping the hexagonal faces of this truncated tetrahedron; a metal atom on an 8(c) site (C) lies at the polyhedron center. Three kinds of interstices are formed between adjacent polyhedra: one, centered at (0,0,0; *etc.*) and bounded by a cubo-octahedron of atoms on 48(h) sites, is occupied by a metal atom on a 4(a) site (A); another, centered near ($\frac{1}{4}$,0,0; *etc.*) and bounded by a square antiprism of atoms on 48(h) and 32(f) sites, is occupied by a carbon atom on a 24(e) site; the third, centered at ($\frac{1}{2},\frac{1}{2},\frac{1}{2}$; *etc.*) and bounded by a cube of atoms on 32(f) sites, is empty.

τ carbides precipitated from multicomponent alloys generally contain more than one metallic element, although an element that forms a stable binary τ carbide (*e.g.* Cr or Mn) often predominates. Since the four symmetry sites available to metal atoms differ in their coordination numbers, coordination geometries, and proximity to carbon, one may anticipate non-random elemental distributions on them due to variations in atomic sizes and chemical affinities. The long-range components of such distributions are determined with relative ease from Bragg X-ray diffraction data when the number of metallic elements is small (usually two) and when their X-ray scattering factors differ appreciably. Thus, in the stoichiometric phases $(Fe_{21}W_2)C_6$ and $(Fe_{21}Mo_2)C_6$, the large atoms tungsten and molybdenum are found exclusively on 16-coordinated 8(c) sites at Friauf polyhedra centers (Stadelmeier, 1969).

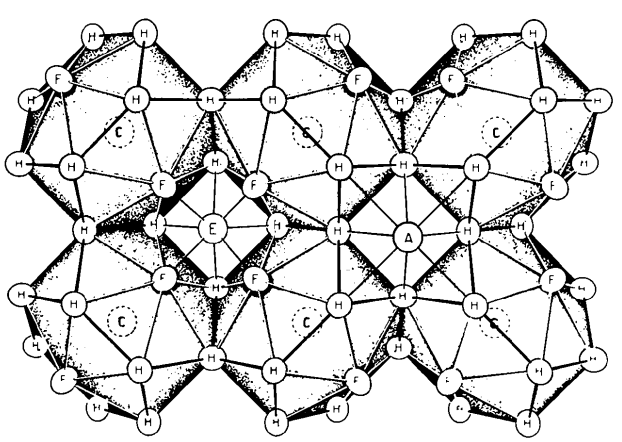

Fig. 1. A typical τ-carbide structure viewed along a cube axis with the other cube axes vertical and horizontal. Atoms are labeled to correspond to the Wyckoff notations of the five occupied symmetry sites. They have boundaries that each enclose a volume in which there is a 99·999% probability of finding the depicted atom for the crystal with $x = 7{\cdot}3_6$. Thick solid bonds outline truncated tetrahedral faces of Friauf polyhedra; open bonds connect atoms (H) at the corners of these faces to face-capping atoms (F). Atoms (C) with dotted outlines are at polyhedra centers. Thin solid bonds connect atoms in interstices of the polyhedral network to near neighbors. The distance between a metal atom in a 4(a) site (A) and a carbon atom in a 24(e) site (E) is about one-fourth of a unit-cell edge.

The metal-atom X-ray scattering factors in some bimetallic τ carbides of practical importance do not differ appreciably, yet other kinds of experiments (*e.g.* neutron diffraction or Mössbauer spectroscopy) have not been performed in order to estimate long- or short-range distribution parameters. An example is the solid solution of iron in $Cr_{23}C_6$, $(Cr_{23-x}Fe_x)C_6$, in which a limiting concentration is reached at $x \simeq 7{\cdot}5$ (Kuo, 1953) under conditions approaching equilibrium.* Since the sizes of Fe and Cr atoms are nearly the same, it would be difficult to predict distribution parameters at any value of x, though specific values of these parameters and their variation with x could be a factor in the eventual destabilization of the phase.†

The present paper describes collections and analyses of single-crystal Bragg X-ray diffraction data from $(Cr_{23-x}Fe_x)C_6$ τ carbides with $x = 0$, $0{\cdot}7_4$, $1{\cdot}7_0$, $4{\cdot}1_3$, and $7{\cdot}3_6$. While a primary objective of these experiments was to add to the structural description of the carbides themselves, another important objective was to test and compare the possibilities of recovering statistically and physically meaningful estimates of long-range metal-atom distribution parameters from (a) extensive data sets precisely measured with conventional Mo $K\alpha$ X-radiation, and (b) less extensive data sets collected with edge-tuned synchrotron radiation (SR) that enhances atomic scattering factor differences through anomalous disperson. The experiments parallel a similar study of long-range site preferences in σ phases (Yakel, 1983*a*,*b*).

The following section gives details of specimen preparation, data collection, reduction, and analysis. Results are then presented and discussed in view of the experimental objectives stated above. Conclusions reported here confirm preliminary findings noted in an earlier communication concerning their metallurgical significance (Yakel, 1982).

* Higher iron contents (approaching $x \simeq 12$) in purportedly $(Cr_{23-x}Fe_x)C_6$ carbides were claimed by Glowacki, Baer & Leda (1968). The phases were found in annealed high-chromium steels that had been austenitized for times up to 1 h at 1173–1323 K. Given the presence of other elements in the steel (notably Si, Mn and Ni) and the conditions of formation of the carbides, one may question the significance of these results to the work reported here.

† Borlera & Pradelli (1971) and Burdese, Pradelli & Gianoglio (1977) inferred non-random distributions in solutions of iron in $Cr_{23}(C_{4{\cdot}5}B_{1{\cdot}5})$ from the value of the limiting solubility and variations of lattice parameter with composition. They also mention an ordering in $(Cr_{23-x}Fe_x)C_6$ solutions that was supposedly suggested by Westgren (1933), but a careful reading of Westgren's paper does not support this inference. The conclusion that solute atoms in such solid solutions segregate to symmetry sites whose total multiplicity is 92 times the observed solubility limit is a dubious extrapolation from the distribution parameters that characterize discrete phases such as $(Fe_{21}Mo_2)C_6$.

Table 1. *Results of chemical analyses, lattice-parameter measurements, estimates of crystal volumes, and data collection conditions and statistics for* $(Cr_{23-x}Fe_x)C_6$ *τ-carbide crystals*

E.s.d.'s in the first three quantities are given in parentheses.

	$x=0$	$0{\cdot}7_4$ (0_8)	$1{\cdot}7_0$ (0_4)	$4{\cdot}1_3$ (0_6)	$7{\cdot}3_6$ (0_9)
Analysis					
Wt.% Fe	—	—	$7{\cdot}4_5$ (1_0)	$17{\cdot}9_6$ (1_0)	$31{\cdot}7_2$ (1_0)
Wt.% Cr	—	—	$86{\cdot}9_0$ (1_0)	$76{\cdot}4_2$ (1_0)	$62{\cdot}7_2$ (1_0)
a_0 (Å) [$T=293(0{\cdot}5)$ K]	10·6595 (4)	10·6537 (1)	10·6454 (6)	10·6199 (3)	10·5966 (3)
Crystal volume ($10^4\times\mu m^3$)	2·3(8)	9·3 (8)	2·4 (8)	3·6 (8)	2·2 (8)
2θ scan width (°)	1·1	1·1	1·0	1·0	0·8
Counting time/step (s)	2·5	2-3·5	3	2	2-3
Total No. of reflections measured	1801	2429	2477	1793	1148
$\bar{\sigma}$*	0·06	0·04	0·04	0·05	0·07
No. of reflections with $I>\sigma(I)$	1378	2155	1934	1471	975
No. of reflections with $I>2\sigma(I)$	1097	1943	1598	1305	869

$$* \bar{\sigma}=[(1/N_0)\sum_{n=1}^{N_0} I_n/\sigma(I_n)]^{-1}.$$

Experimental

(*a*) *Specimen preparation and characterization*

τ-carbide crystals were precipitated from Cr-C and Cr-Fe-C alloys by heat treatments of as-cast ingots for several hundred hours at 1473 K. Ternary alloy compositions were chosen to yield approximately the desired Cr:Fe atom ratios in the carbides based on the equilibrium diagram reported by Bungardt, Kunze & Horn (1958). After dissolution of the matrix metal, the precipitates were characterized by X-ray powder diffraction,* by optical microscopy, and, for all save the phases with $x=0$ and $0{\cdot}7_4$, by chemical analyses for chromium and iron. The results are summarized in Table 1.

No phase other than the cubic τ carbide was found in any preparation. All chemical analyses were consistent with the general $M_{23}C_6$ formula if differences between total sample weights and analyzed weights of chromium and iron were ascribed to carbon. Average crystal sizes were larger (up to 150 μm diameter) and morphologies better developed at higher iron concentrations. Tablet-like crystals with partial hexagonal outlines were frequently observed. Fig. 2 shows that the measured lattice parameters of the four τ solid solutions decrease almost linearly with increasing iron content from the value found for $Cr_{23}C_6$. Lattice parameters measured at $x=7{\cdot}3_6$ and $1{\cdot}7_0$ are in substantial agreement with those reported at comparable compositions by Shaw & Quarrell (1957) and by Westgren, Phragmén & Negresco (1928); that found for $Cr_{23}C_6$ is in excellent agreement with the value reported by Westgren (1933).† The composition of the phase with $x=0{\cdot}7_4$ was inferred from its measured lattice parameter.

(*b*) *Diffraction data collection*

Crystals in the 40–70 μm diameter size range were selected from each carbide preparation and mounted suitably. Rotation and Weissenberg photographs exposed with Ni-filtered Cu $K\alpha$ X-radiation were used to verify crystal quality and to determine approximate orientations of crystallographic axes relative to mounting fiber directions.

An automated Picker four-circle diffractometer in bisecting geometry was used for all diffraction data collections with conventional Mo $K\alpha$ X-radiation [$\lambda(K\alpha_1)=0{\cdot}70930$ Å]. Orientation matrix elements were determined by least-squares fits of observed centering angles of $K\alpha_1$ components of 12 reflections in the 107–118° 2θ range. Estimated lattice parameters (constrained to cubic symmetry) at 293 (0·5) K were invariably within one or two standard deviations of

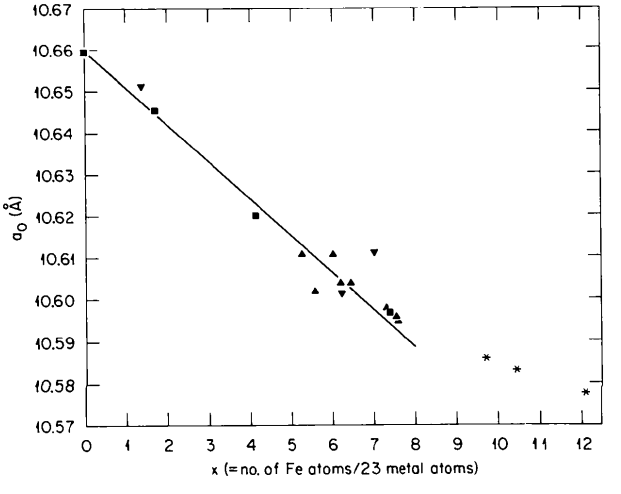

Fig. 2. Measured lattice parameters of $(Cr_{23-x}Fe_x)C_6$ τ carbides as a function of x: ■, present work, measured Cr and Fe composition; ▲, Shaw & Quarrell (1957), measured Cr and Fe composition; ▼, Westgren, Phragmén & Negresco (1928), measured Cr and C composition; *, Glowacki, Baer & Leda (1968), measured Cr composition. Probable errors in parameters and compositions for the ■ data are smaller than the printed symbols. The straight line is a linear fit to the ■ data ($a_0=10{\cdot}6599-0{\cdot}00894x$ Å).

* Powder diffraction patterns were recorded at 293 (1) K with V-filtered Cr $K\alpha$ X-radiation [$\lambda(K\alpha_1)=2{\cdot}28970$ Å] in 114·6 mm diameter Debye-Scherrer cameras using the Straumanis film arrangement. Lattice parameters were computed from measurements of 12–14 high-angle interplanar spacings ($119\leq 2\theta\leq 166°$) fitted with Nelson-Riley extrapolation functions.

† All previously reported parameters have been converted to currently accepted Å units by multiplication by 1·00202.

the powder diffraction values listed in Table 1. Integrated intensities of Bragg reflections up to 130° 2θ were measured with $\theta/2\theta$ scans (step = 0·01° 2θ) under the conditions summarized in Table 1. All index triples consistent with face centering of the lattice were included for at least 3 or 4 sets of equivalent reflections. Dimensions of crystals from which data had been recorded were measured with an estimated precision of ±3 μm in preparation for absorption corrections to the data.

The carbide crystal with $x = 0{\cdot}7_4$ from which conventional data had been collected was also the subject of SR diffraction experiments. This work was carried out at the Stanford Synchrotron Radiation Laboratory with an automated CAD-4 diffractometer on an unfocused beam line. General conditions for the experiment included a stored electron energy of 3 GeV with currents up to 100 mA, Si (111) incident-beam monochromators detuned to reduce third-order harmonic contributions, and an He- or He,N_2-filled ionization chamber that monitored the monochromated incident X-ray intensity. Measurements of Cr K and Fe K absorption profiles from powdered specimens of this carbide gave edge energies at 5990 and 7112 eV, respectively, compared to 5989 and 7111 eV for the elements (*International Tables for X-ray Crystallography*, 1974). Integrated intensities of allowed Bragg reflections at scattering angles up to 140° 2θ were recorded with $\theta/2\theta$ scans at X-ray energies of 5986, 5988 and 7107 eV (all energies have e.s.d.'s of ±1 eV). Confidence in these energy values was increased by the fact that wavelengths corresponding to them (conversion factor = 12398·1 eV Å), coupled with observed scattering angles of 18 centered reflections, gave the same lattice parameter for this crystal as had been measured in the conventional diffraction experiments, *i.e.* 10·6535 (3) Å.

(*c*) *Data reduction and analysis*

Physical constants, mass absorption coefficients (Mo $K\alpha$), atomic scattering factors at the high-energy limit, and dispersion corrections to these factors (Mo $K\alpha$) were taken from *International Tables for X-ray Crystallography* (1974). Absorption coefficients for energies at which synchrotron-radiation diffraction data had been collected were estimated by extrapolation of tabulated values. Dispersion corrections at these energies, computed with the Cromer & Liberman (1970) method as modified by Cromer (1983), are listed in Table 2. The suggested uncertainties included with computed terms near absorption edges reflect only uncertainties in photon energy and not possible variations due to the fact that the absorbers are bound atoms.

Conventional X-ray diffraction data were reduced to relative $F^2_{obs}(hkl)$ values in the usual manner. Corrections for absorption employed the *ORABS* algorithm (Shoemaker, 1966; accession No. 362) with polyhedral crystal shapes. Parameters intended to describe isotropic extinction effects (Coppens & Hamilton, 1970) were included in the last stages of least-squares calculations with replicate-averaged data sets. Corrections for extinction based on these parameters were then made to all data (including synchrotron-radiation diffraction data) before averaging symmetry equivalents. Other details of the reduction of conventional X-ray and synchrotron-radiation diffraction data sets duplicate those reported previously (Yakel, 1983*a*).

Table 2. *Calculated dispersion terms for* Fe, Cr *and* C *at synchrotron-radiation energies used for collection of data from the* $(Cr_{22\cdot3_6}Fe_{0\cdot7_4})C_6$ *τ-carbide crystal*

Dispersion terms calculated by the method of Cromer & Liberman (1970) as modified by Cromer (1983).

Energy (keV)	5986 (1)	5989 (1)	7107 (1)
Wavelength (Å)	2·0713 (3)	2·0703 (3)	1·7446 (2)
f'_{Fe} (e)	−1·70	−1·70	−7·1 (2)*
f''_{Fe} (e)	0·64	0·64	0·47
f'_{Cr} (e)	−7·5 (2)	−9·2 (8)	−0·80
f''_{Cr} (e)	0·46	0·46	2·99
f'_{C} (e)	0·03	0·03	0·02
f''_{C} (e)	0·02	0·02	0·01

* Suggestions of errors reflect only the estimated uncertainties in photon energies. Where no error is stated, the calculated term given does not change significantly in the likely range of photon energy.

The starting model for each τ-carbide crystal studied was the $Cr_{23}C_6$ structure derived by Westgren (1933). At a given value of x this model has three variable atomic coordinates [one each for atoms in 24(e), 32(f) and 48(h) sites], a maximum of nine variable thermal parameters if anisotropic vibrations are assumed, and, for a bimetallic carbide, three variable metal-atom site-occupation parameters. In constraining the refinement to only three distribution parameters, one assumes that compositions are known, that constitutional vacancies do not occur in significant numbers, and that atomic coordinates and thermal vibration parameters of an atom at a given symmetry site are the same whether that site be occupied by a Cr or an Fe atom. Site-occupation parameters for the starting model were random values corresponding to the value of x.

In each case, refinement of the starting model parameters was accomplished by full-matrix least-squares calculations that minimized the sum of squares of differences between weighted observed and calculated $F^2(hkl)$ values. Weights of the former were reciprocals of variances assigned according to $\sigma^2[F^2_{obs}(hkl)] = \sigma^2_{cs}(hkl) + [qF^2_{obs}(hkl)]^2$, where $\sigma^2_{cs}(hkl)$ was the variance computed from counting statistics alone, and q, an 'ignorance' factor (Corfield, Doedens & Ibers, 1967), was chosen to be 0·024–0·030 for the conventional data sets and 0·057 for the SR data sets based on standard statistical tests during subsequent refinement procedures (*International Tables for X-ray Crystallography*, 1974).

Table 3. *Final values of variable atom coordinates, thermal vibration and site-occupation parameters for structural models of* $(Cr_{23-x}Fe_x)C_6$ *τ carbides, including relative changes in configurational entropies (metal-atom sites only) computed from the latter*

Estimated standard deviations in the last significant figures are given in parentheses. Parameters $b_{ij} = \beta_{ij} \times 10^{-4}$ appear in temperature-factor expressions of the form $\exp(-h^2b_{11} - k^2b_{22} - l^2b_{33} - 2hkb_{12} - 2hlb_{13} - 2klb_{23})$. Parameters in square brackets ($x = 0$) are those reported by Westgren (1933). Metal-atom site-occupation parameters are given as the probability, p_{Fe}, that a randomly selected site will be occupied by an iron atom; a chromium atom occupies the site with probability $(1 - p_{Fe})$. Any three of the four site-occupation parameters may be independently varied, the fourth being calculated from them and the known composition. The listed e.s.d. for a given site-occupation parameter was computed from least-squares calculations in which that parameter was independently varied. Site-occupation parameters for the crystal with $x = 0{\cdot}7_4$ include results of analyses with conventional (con) and SR diffraction data, and weighted averages of the two. For analyses with SR data near the Cr K edge, the $f'_{Cr}[(\sin\theta)/\lambda]$ functional parameters C and M were:

E (eV)	5989 (1)	5986 (1)
C (e)	−8·7 (4)	−8·2 (3)
M (Å^2)	1·0 (3)	1·1 (2).

Entropy changes are given as the increase per 92 metal atoms divided by kn; changes corresponding to random site-occupation parameters are included.

Atom	Site symmetry	Wyckoff notation	Parameter	$x = 0$	$0{\cdot}7_4$	$1{\cdot}7_0$	$4{\cdot}1_3$	$7{\cdot}3_6$
A	*m3m*	4(*a*)	β_{11}	11·9 (4)	11·7 (2)	8·7 (2)	8·3 (2)	9·2 (3)
			p_{Fe}(con)	—	0·30 (5)	0·86 (6)	0·95 (7)	1·00 (4)
			(SR)		0·26 (1)			
			(av)		0·27 (3)			
C	$\bar{4}3m$	8(*c*)	β_{11}	8·0 (2)	8·0 (1)	7·7 (1)	9·0 (2)	11·3 (2)
			p_{Fe}(con)	—	0·10 (4)	0·20 (4)	0·28 (5)	0·35 (5)
			(SR)		0·04 (1)			
			(av)		0·05 (3)			
F	3*m*	32(*f*)	X	0·38199 (2), [0·385]	0·38195 (1)	0·38181 (2)	0·38177 (2)	0·38173 (2)
			β_{11}	7·4 (1)	6·84 (6)	6·37 (7)	6·92 (7)	8·3 (1)
			β_{12}	1·3 (1)	0·91 (5)	1·10 (8)	1·46 (8)	1·5 (1)
			p_{Fe}(con)	—	0·00 (2)	0·02 (2)	0·08 (2)	0·22 (3)
			(SR)		0·022 (5)			
			(av)		0.02 (2)			
H	*mm*	48 (*h*)	X	0·16991 (2), [0·165]	0·16943 (1)	0·16857 (2)	0·16839 (2)	0·16852 (2)
			β_{11}	7·8 (2)	7·4 (1)	7·0 (1)	7·9 (1)	9·0 (2)
			β_{22}	6·5 (1)	6·29 (6)	5·70 (8)	5·86 (8)	6·9 (1)
			β_{23}	0·7 (1)	0·75 (6)	0·4 (1)	0·4 (1)	0·4 (1)
			p_{Fe}(con)	—	0·01 (2)	0·02 (2)	0·16 (1)	0·33 (2)
			(SR)		0·018 (6)			
			(av)		0·02 (2)			
E (carbon)	4*mm*	24 (*e*)	X	0·2751 (3), [0·275]	0·2760 (2)	0·2765 (2)	0·2766 (2)	0·2766 (3)
			β_{11}	12 (2)	8·8 (9)	11 (1)	9 (1)	11 (2)
			β_{12}	7 (1)	6·9 (6)	8·1 (8)	9·7 (8)	11 (1)
			$\Delta S/kn$ (calc)	0	11 (2)	13 (2)	36 (3)	52 (3)
			$\Delta S/kn$ (rand)	0	13·1	24·3	43·3	57·3

Refinements of the starting model based on conventional X-ray diffraction data sets were carried out in successive stages, starting with a scale and overall temperature factor, expanding to include variable atomic coordinates and increasingly complex descriptions of thermal vibrations of individual atoms, and finally adding the variable site-occupation parameters. Data with $(\sin\theta)/\lambda \le 0{\cdot}35$ Å^{-1} were excluded from refinements in which site-occupation parameters were varied to minimize charge-transfer effects. Hypothesis tests (Hamilton, 1965) were used to evaluate the statistical significance of improvements in appropriate measures of agreement at all stages of the refinements. Convergence was achieved in every case, parameter changes after the final least-squares cycles invariably being either zero or small fractions of estimated standard deviations.

The refinement of the starting model based on SR diffraction data sets from the crystal with $x = 0{\cdot}7_4$ included site-occupation parameters and scale factors only. All other variable parameters were fixed at values given by the refinement based on the conventional data set. Least-squares calculations with data collected near the Cr K-edge energy gave results suggesting that improved agreement between observed and computed $F^2(hkl)$ values would be produced if f'_{Cr} were allowed to have a functional dependence on $(\sin\theta)/\lambda$. The function chosen was $f'_{Cr} = -C\exp[-M(\sin^2\theta)/\lambda^2]$. Since the least-squares program used (*XFLS*, Shoemaker, 1966; accession No. 389) did not allow for the straightforward addition of extra parameters describing this proposed dependence, repeated refinements with a series of C and M trial values were made. Those giving minimum agreement factors were readily found but quantitative estimates of errors in them were not directly calculable. Qualitative estimates are included with the values for C and M tabulated in the next section as indicators only. Note that the same trends were *not* observed in the course of least-squares calculations with data collected near the Fe K-edge energy. This suggests that the effect at the Cr K edge is more probably due to the proposed $(\sin\theta)/\lambda$ dependence of f'_{Cr} than to incorrectly assigned thermal vibration or extinction parameters.

Results and discussion

(*a*) *Atomic coordinates and distribution parameters*

Table 3 presents final values of all varied parameters and estimates of their standard deviations

Table 4. *Measures of agreement from final least-squares refinement cycles with structural models of* $(Cr_{23-x}Fe_x)C_6$ *τ carbides*

N is the number of observations used to refine p parameters of the model. Measures of agreement are the usual ones defined by crystallographers [see, *e.g.* Brown & Chidambaram (1969)].

(*a*) Conventional Mo $K\alpha$ diffraction data

	$x=0$	$0{\cdot}7_4$	$1{\cdot}7_0$	$4{\cdot}1_3$	$7{\cdot}3_6$
N	495	556	518	523	449
p	13	16	16	16	16
$R(F^2)$	0·0315	0·0173	0·0275	0·0245	0·0237
$wR(F^2)$	0·0391	0·0387	0·0353	0·0428	0·0445
σ_1	1·0632	1·0836	1·1251	1·0535	1·0606
p^*	—	13	13	13	13
$R(F^2)$	—	0·0198	0·0295	0·0435	0·0483
$wR(F^2)$	—	0·0427	0·0395	0·0673	0·0716
σ_1	—	1·1535	1·2210	1·1264	1·1310

(*b*) SR diffraction data ($x=0{\cdot}7_4$)

Conditions	N	p†	wR	σ_1
(1) $f'_{Cr}=C\exp[-M(\sin^2\theta)/\lambda^2]$ at 5986 and 5989 eV; $f'_{Fe}=-7{\cdot}1$ e (Cromer, 1983) at 7107 eV	133	3	0·0669	1·3198
(2) Refined constant f'_{Cr} ($=-6{\cdot}73$ e at 5986 eV, $=-7{\cdot}20$ e at 5989 eV); $f'_{Fe}=-7{\cdot}1$ e at 7107 eV	133	5	0·1377	2·7174
(3) Nonvariable constant f'_{Cr} and f'_{Fe} from Table 2	133	3	0·2241	4·4219
(4) $f'_{Cr}=C\exp[-M(\sin^2\theta)/\lambda^2]$ at 5986 and 5989 eV; $f'_{Fe}=-7{\cdot}1$ e at 7107 eV; site-occupation parameters constrained to random values	133	0†	0·1600	3·1155
(5) $f'_{Cr}=-8{\cdot}2$ e $[\exp(-1{\cdot}1\sin^2\theta/\lambda^2)]$ at 5986 eV	39	3†	0·0649	1·8424
(6) Refined constant f'_{Cr} ($=-6{\cdot}73$ e) at 5986 eV	39	4	0·1630	4·6247
(7) $f'_{Cr}=-8{\cdot}7$ e $[\exp(-1{\cdot}0\sin^2\theta/\lambda^2]$ at 5989 eV	39	3†	0·0846	2·2320
(8) Refined constant f'_{Cr} ($=-7{\cdot}20$ e) at 5989 eV	39	4	0·1699	4·4835
(9) $f'_{Fe}=-7{\cdot}1$ e at 7107 eV	55	3	0·0488	1·0256

* Metal-atom site-occupation parameters are constrained to random values.

† Unless noted under Conditions, three metal-atom site-occupation parameters are always varied. Additional variable parameters are constant f'_{Cr} values, *i.e.* values that are not a function of $(\sin\theta)/\lambda$. In case (4), no parameters were varied and the measures of agreement resulted from a structure-factor calculation alone. Values of C and M selected for 5986 and 5989 eV data are listed in the footnote to Table 3 and are repeated for cases (5) and (7).

produced by the least-squares calculations described above.* Atomic coordinates reported by Westgren (1933) for $Cr_{23}C_6$ are included in the parameter list for $x=0$. Table 4(*a*) gives measures of agreement computed by final refinement cycles for Mo $K\alpha$ data with models having variable metal-atom site-occupation parameters and (for $x\neq 0$) with models having these parameters constrained to chemical-average values. Agreement factors for the $x=0{\cdot}7_4$ composition are listed in Table 4(*b*) for final refinement cycles using SR data sets alone with various conditions placed on f'_{Cr}.

The most prominent features of the difference Fourier maps generated with structure factors calculated from final parameter values listed in Table 3 were positive and negative peaks corresponding to densities of $\pm 0{\cdot}1$ e Å^{-3} near carbon-atom sites. Such features were observed for all crystals studied. Models in which 24(*e*) site-occupation parameters were allowed values ≤ 1 did not produce significant improvements in measures of agreement.

In order to assess the significance of the metal-atom distribution parameters in Table 3, one may make the null hypothesis that the observed diffraction data are fitted as well by a structural model with chemical-average distributions as they are by a model with variable distributions. Appropriate ratios of wR or σ_1 at each composition with $x\neq 0$ show that this null hypothesis can be rejected with a chance of error of less than 1% (Hamilton, 1965).

Results for the phase with $x=0{\cdot}7_4$ indicate a rather surprising sensitivity of the conventional Mo $K\alpha$ data to the distribution parameters even though the Fe/Cr atom ratio is only $0{\cdot}03_3$. Moderately good agreement of these parameters with the more precise values produced by models fitted to the SR data sets supports the supposition that the sensitivity is real and not due to unsuspected artifacts in the conventional data. Together with reported results for Cr–Fe σ phases (Yakel, 1983*a*), the conclusions reached here suggest that one may generally derive physically significant long-range distribution parameters from analyses of extensive, precise, conventional Bragg X-ray diffraction data collected from bimetallic Cr–Fe phases with about five or fewer sites available for metal-atom occupation. For Cr and Fe in the range $0\leq(\sin\theta)/\lambda\leq 1{\cdot}2$ Å^{-1}, $\Delta f^0/f^0_{av}\simeq 0{\cdot}06$–$0{\cdot}11$, where $f^0_j=f_j-f'_j-if''_j$, $f^0_{av}=\frac{1}{2}(f^0_{Fe}+f^0_{Cr})$ and $\Delta f^0=f^0_{Fe}-f^0_{Cr}$.

A plot of the distribution parameters for the four metal-atom sites as a function of x (Fig. 3) illustrates

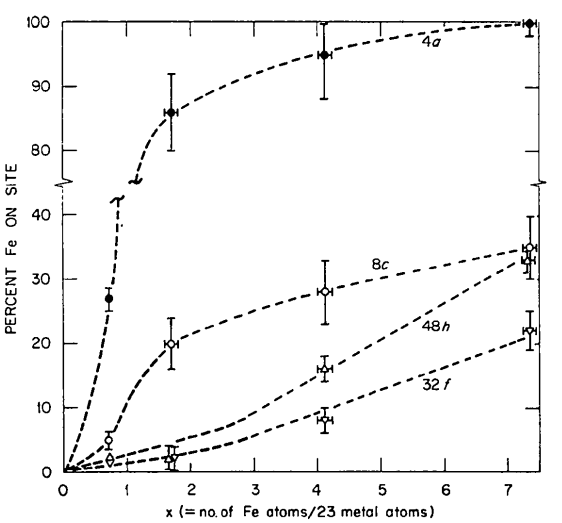

Fig. 3. Variations with x of site-occupation parameters of iron on the four independent symmetry sites that are occupied by metal atoms in $(Cr_{23-x}Fe_x)C_6$ τ carbides. Dashed curves are meant as a help to the viewer only.

* Lists of observed and calculated squares of structure factors (with estimated standard deviations of the former) have been deposited with the British Library Document Supply Centre as Supplementary Publication No. SUP 43766 (28 pp.). Copies may be obtained through The Executive Secretary, International Union of Crystallography, 5 Abbey Square, Chester CH1 2HU, England.

the physical significance of the results. The substitution of iron for chromium atoms is not random, but shows a marked preference for the geometrically close-packed 4(a) sites and, at lower x values, for the Friauf polyhedra centers [8(c) sites]. Atoms at either set of preferred sites are not within bonding distance of carbon atoms. Atoms at sites less favorable for iron substitution are bonded to carbon atoms, those at 48(h) sites forming two bonds, those at 32(f) sites forming three. It seems probable that the replacement of strong Cr–C bonds with relatively weaker Fe–C bonds is the primary factor raising the free energy of the τ solid solution to the point of instability.

One may reasonably ask why the iron-atom occupation probability at 8(c) sites saturates at about 35% when filling these sites could reduce the need to substitute iron in carbon-bonded sites as x increases. The answer is not obvious but may lie in a description of bonding states in the Friauf polyhedron.

A configuration entropy increment, $\Delta S/kn$,* due to the measured metal-atom distribution parameters is easily calculated at each composition studied. Values are included in Table 3, together with maximum entropy increments for random occupation of all sites.

(*b*) *Interatomic distances*

Tables 5 and 6 give values of distances D_{ij}^r between near-neighbor atoms i and j for crystals of composition $r = 0, 1, 2, 3$, and 4, corresponding to $x^r = 0, 0{\cdot}7_4, 1{\cdot}7_0, 4{\cdot}1_3$, and $7{\cdot}3_6$, respectively. Table 5 includes a complete description of the environment of each atom together with bond orders computed from Pauling's (1960) relationship. Several general observations concerning these distances at any given value of x^r merit attention.

(1) While the coordination number of an atom at an 8(c) site is 16, the four face-capping F atoms of a Friauf polyhedron are closer to the central atom by almost 0·5 Å than are the twelve H atoms that define the truncated tetrahedron; corresponding bond orders are in the ratio 6:1.

(2) The distance between a carbon atom and one set of its nearest neighbors (F atoms) is significantly shorter (by 0·02 Å) than the distance to the other set (H atoms).

(3) Distances between H atoms on the surface of a truncated tetrahedron occur in two sets: a short distance along an edge shared by two adjacent Friauf polyhedra, and a distance that is longer by ~0·1 Å that also defines the edge of a cubo-octahedron about an A atom.

(4) The six distances between a face-capping F atom and the H atoms defining the capped face of a Friauf polyhedron are longer by ~0·1 Å than the contacts between the latter.

(5) The F atoms from eight different Friauf polyhedra enclose a cubic interstice whose size changes but little over the entire range of x values. The average radius of the interstice is 0·92 Å; it is large enough to accommodate a carbon atom but, as difference maps show, it does not do so at any composition.

While systematic changes in the interatomic distances with x may be inferred from the lists in Tables 5 and 6, it is more instructive to ask how the variations compare with the linear decrease of the measured lattice parameter a^r as x increases. A parameter that would reflect such relative changes can be defined at any of the compositions studied with $r > 0$ as:

$$Q_{ij}^r = [(\Delta D_{ij}^r/\Delta x^r)/(\Delta a^r/\Delta x^r)](a^r/D_{ij}^r)$$
$$= (\Delta D_{ij}^r/D_{ij}^r)/(\Delta a^r/a^r)$$
$$= \Delta \ln (D_{ij}^r)/\Delta \ln (a^r),$$

where $\Delta p^r = p^r - p^{r-1}$ for $p \equiv D_{ij}$, a, or x. Positive values of Q_{ij}^r indicate the ijth interatomic distance decreases with increasing x at a rate less than, equal to, or greater than that of the lattice parameter if $0 \le Q_{ij}^r < 1, = 1, > 1$, respectively; negative values of Q_{ij}^r indicate that, conversely to the dependence of a on x, the distance increases with increasing x. Since the compositions of the crystals studied are not closely spaced, the discrete values of Q_{ij}^r listed in Table 6

Table 5. *Near-neighbor interatomic distances and bond orders for* $Cr_{23}C_6$

Estimated standard deviations in the last significant figures are given in parentheses.

Atom on site i	Atom on site j	N_{ij}*	D_{ij}^0 (Å)	Bond order†
A	H	12	2·5613 (3)	0·48
	E (carbon)	6	2·933 (3)	0·02
				$\sum(A) = 5{\cdot}95$
C	F	4	2·4369 (4)	0·78
	H	12	2·9256 (2)	0·12
				$\sum(C) = 4{\cdot}55$
H	E (carbon)	2	2·130 (2)	0·52
	H	1	2·4148 (6)	0·85
	A	1	2·5613 (3)	0·48
	H	4	2·5613 (3)	0·48
	F	4	2·6456 (2)	0·35
	C	2	2·9256 (2)	0·12
				$\sum(H) = 5{\cdot}94$
F	E (carbon)	3	2·113 (2)	0·55
	C	1	2·4369 (4)	0·78
	F	3	2·5159 (5)	0·58
	H	6	2·6456 (2)	0·35
				$\sum(F) = 6{\cdot}26$
E (carbon)	F	4	2·113 (2)	0·55
	H	4	2·130 (2)	0·52
	A	1	2·933 (3)	0·02
				$\sum(E) = 4{\cdot}30$

* N_{ij} is the number of atoms j at distance D_{ij}^0 from atom i.

† Bond orders are computed from Pauling's (1960) relationship with $R_1(\text{Cr}) = 1{\cdot}186$ Å, $R_1(\text{carbon}) = 0{\cdot}772$ Å. $\sum(i) = \sum_j N_{ij} \times (\text{bond order})_{ij}$ for the atom i.

* Here, k is Boltzmann's constant and ΔS is the entropy increment due to Cr–Fe mixing on the metal-atom sites in n unit cells.

Table 6. *Selected interatomic distances and Q^r_{ij} values for* $(Cr_{23-x}Fe_x)C_6$ *τ carbides*

Estimated standard deviations in the last significant figures are given in parentheses. See text for definition of Q^r_{ij}.

Atom on site i	Atom on site j	$x=0$ D^0_{ij} (Å)	$0{\cdot}7_4$ D^1_{ij} (Å)	Q^1_{ij}	$1{\cdot}7_0$ D^2_{ij} (Å)	Q^2_{ij}	$4{\cdot}1_3$ D^3_{ij} (Å)	Q^3_{ij}	$7{\cdot}3_6$ D^4_{ij} (Å)	Q^4_{ij}
A or *H*	*H**	2·5613 (3)	2·5526 (2)	6 (1)	2·5378 (3)	8 (1)	2·5290 (3)	1·5 (2)	2·5254 (3)	0·6 (2)
H	*H*†	2·4148 (6)	2·4279 (4)	−10 (1)	2·4519 (5)	−13 (1)	2·4513 (5)	0·1 (2)	2·4422 (6)	1·7 (2)
F	*H*	2·6456 (2)	2·6471 (1)	−1·0 (2)	2·6502 (2)	−1·5 (2)	2·6449 (2)	0·8 (1)	2·6379 (2)	1·4 (1)
F	*F*	2·5159 (5)	2·5154 (3)	0·4 (4)	2·5164 (4)	−0·4 (4)	2·5112 (4)	0·8 (1)	2·5066 (5)	0·8 (1)
C	*F*	2·4369 (4)	2·4347 (2)	1·8 (4)	2·4303 (4)	2·2 (4)	2·4238 (3)	1·1 (1)	2·4177 (4)	1·1 (2)
C	*H*	2·9256 (2)	2·9270 (1)	−0·8 (2)	2·9301 (2)	−1·4 (2)	2·9242 (1)	0·84 (6)	2·9170 (1)	1·13 (8)
E (carbon)	*F*	2·113 (2)	2·106 (1)	5 (2)	2·103 (1)	2 (1)	2·098 (1)	1·0 (4)	2·093 (2)	1·0 (5)
E (carbon)	*H*	2·130 (2)	2·133 (1)	−2 (2)	2·131 (1)	1 (1)	2·126 (1)	1·0 (4)	2·122 (2)	0·9 (5)
E (carbon)	*A*	2·933 (3)	2·941 (2)	−5 (3)	2·944 (3)	−1 (1)	2·937 (3)	0·7 (5)	2·931 (3)	1·1 (7)

* This H–H distance is a Friauf polyhedron edge that also serves as an edge of a cubo-octahedron about an *A* atom.
† This H–H distance is a Friauf polyhedron edge that is shared with another Friauf polyhedron.

cannot give more than a qualitative suggestion of the behaviors of the continuous functions $Q_{ij}(x)$. Nevertheless, two general features of these behaviors may be deduced.

(1) In the range $0 \le x \le 2$, the responses of the several Q_{ij} to increasing x vary from decreases that are 6–8 times the rate of overall lattice contraction to increases that are over 10 times the absolute value of that rate. One may interpret these responses as a tendency for interatomic contacts to shorten between all atoms in the geometrically close-packed cubo-octahedron surrounding the 4(*a*) site, between the *C* atom at the Friauf polyhedron center and its four nearest *F*-atom neighbors, and between the carbon atom and its bonded neighbors [especially those on 32(*f*) sites]. As a consequence of these contractions, the short edge shared between two Friauf polyhedra increases in length significantly while the remaining distances in the Friauf polyhedron increase slightly. These changes may be correlated with effects on bonding energy due to preferential site occupation by iron atoms. However, changes in calculated bond orders with x are too small to have obvious significance.

(2) In the range $4 \le x \le 7{\cdot}4$, $Q_{ij}(x)$ approaches a value near one for all *ij* near-neighbor atom pairs regardless of the behavior at smaller x. This isotropic contraction at a rate of 0·08% as x nears its high-iron limit increases bond orders at a rate of 0·3% at *A* atoms (where P_{Fe} is not changed with x) to ~1·3% at the other metal-atom sites (where P_{Fe} is still increasing with x).

(*c*) *Angular dependence of* f'_{Cr} *near the* Cr *K edge*

Table 3 lists values of *C* and *M* that give the best fit of the model with $f'_{Cr} = -C \exp[-M(\sin^2\theta)/\lambda^2]$ to SR diffraction data collected from the crystal with $x = 0{\cdot}7_4$ at photon energies of 5986 and 5989 eV. The possible significance of these parameters may be gauged *via* the hypothesis that the observed data are fitted as well by a model with constant f'_{Cr} as by the model with an angle-dependent term. Ratios of *wR* or σ_I values cannot be quantitatively interpreted as implying errors to be feared if the hypothesis is rejected because, as noted above, values for models with angle-dependent f'_{Cr} terms were not calculated from unconstrained linear regressions. However, comparisons of relevant agreement factors listed in Table 4 qualitatively suggest that models with angle-dependent terms must be preferred to those with constant terms, whether the constants be taken from Cromer's computations or obtained through a least-squares procedure.

Note that for the models with angle-dependent dispersion terms f'_{Cr}, *C* [$\equiv f'_{Cr}$ at $(\sin\theta)/\lambda = 0$] at 5986 eV is about 0·5 e lower (algebraically) than Cromer's computed value while at 5989 eV it is about 0·5 e higher. Given the ±1 eV uncertainty in the incident X-ray energies, the assumptions inherent in the theory behind Cromer's calculations, and the fact that statistically valid e.s.d.'s are not available for the measured numbers, one cannot attach significance to these differences in *C* as confidently as one can to the departure of *M* from zero at both SR energies.

A similar angular variation in the real part of the dispersion term for samarium near its L_{III} absorption edge was reported by Templeton, Templeton, Phizackerley & Hodgson (1982) through analyses of SR diffraction data from crystals of sodium samarium ethylenediaminetetraacetate octahydrate. If their results are given the same functional dependence on $(\sin\theta)/\lambda$ as that used here, values of $C = -18{\cdot}7$ e and $M = 0{\cdot}80$ Å^2 can be calculated for Sm at 6721 eV (about 5 eV *above* the nominal L_{III}-edge energy). Additional experimental results above and below the absorption edges of other elements are clearly needed before systematic trends can be identified and compared with theoretical predictions.

I am indebted to J. Brynestad, Chemistry Division, Oak Ridge National Laboratory, for preparing the carbides; to W. R. Busing, Chemistry Division, Oak Ridge National Laboratory, for permission to use the automated diffractometer in his laboratory to collect conventional Mo *Kα* diffraction data; to the staff of the Stanford Synchrotron Radiation Laboratory for their support in scheduling the SR diffraction data

collection experiment; and to A. Habenschuss, Oak Ridge Associated Universities, for his help in performing the latter.

References

BORLERA, M. L. & PRADELLI, G. (1971). *Metall. Ital.* **63**, 107-111.
BROWN, G. M. & CHIDAMBARAM, R. (1969). *Acta Cryst.* B**25**, 676-687.
BUNGARDT, K., KUNZE, E. & HORN, E. (1958). *Arch. Eisenhuettenwes.* **29**, 393-394.
BURDESE, A., PRADELLI, G. & GIANOGLIO, C. (1977). *Metall. Ital.* **69**, 487-492.
COPPENS, P. & HAMILTON, W. C. (1970). *Acta Cryst.* A**26**, 71-83.
CORFIELD, P. W. R., DOEDENS, R. J. & IBERS, J. A. (1967). *Inorg. Chem.* **6**, 197-200.
CROMER, D. T. (1983). *J. Appl. Cryst.* **16**, 437.
CROMER, D. T. & LIBERMAN, D. (1970). *Relativistic Calculation of Anomalous-Scattering Factors for X-rays.* Report LA-4403. Los Alamos Scientific Laboratory, New Mexico.
GLOWACKI, Z., BAER, J. & LEDA, H. (1968). *J. Iron Steel Inst.* **206**, 393-394.
HAMILTON, W. C. (1965). *Acta Cryst.* **18**, 502-510.
International Tables for X-ray Crystallography (1974). Vol. IV. Birmingham: Kynoch Press. (Present distributor D. Reidel, Dordrecht.)
KUO, K. (1953). *Jernkontorets Ann.* **137**, 149-156.
LAI, J. K. L. & MESHKAT, M. (1978). *Met. Sci.* **12**, 415-420.
MEINHARDT, D. & KRISEMENT, O. (1962). *Arch. Eisenhuettenwes.* **33**, 493-499.
PAULING, L. (1960). *The Nature of the Chemical Bond*, 3rd ed., pp. 393-448. Ithaca, NY: Cornell Univ. Press.
SAMSON, S. (1964). *The Structure of Metals and Intermetallic Compounds, Sept.* 1, 1953-*Aug.* 31, 1964. Final Report, ONR Contract Nonr-220-33. California Institute of Technology, Pasadena.
SHAW, S. W. & QUARRELL, A. G. (1957). *J. Iron Steel Inst.* **185**, 10-22.
SHOEMAKER, D. P. (1966). *World List of Crystallographic Computer Programs*, 2nd ed. Utrecht: Oosthoek.
STADELMEIER, H. H. (1969). *Metal-Rich Metal-Metalloid Phases*, pp. 141-180, in *Developments in the Structural Chemistry of Alloy Phases*, edited by B. C. GIESSEN. New York: Plenum Press.
TEMPLETON, L. K., TEMPLETON, D. H., PHIZACKERLEY, R. P. & HODGSON, K. O. (1982). *Acta Cryst.* A**38**, 74-78.
WESTGREN, A. (1933). *Jernkontorets Ann.* **117**, 501-512.
WESTGREN, A., PHRAGMÉN, G. & NEGRESCO, TR. (1928). *J. Iron Steel Inst.* **117**, 383-406.
YAKEL, H. L. (1982). *Scripta Metall.* **16**, 453-454.
YAKEL, H. L. (1983*a*). *Acta Cryst.* B**39**, 20-28.
YAKEL, H. L. (1983*b*). *Acta Cryst.* B**39**, 28-33.

Acta Cryst. (1987). B**43**, 238-244

Studies of $K_3Nb_7O_{19}$ by High-Resolution Electron Microscopy and X-ray Powder Diffraction

BY MARGARETA SUNDBERG AND MONICA LUNDBERG

Department of Inorganic Chemistry, Arrhenius Laboratory, University of Stockholm, S-106 91 Stockholm, Sweden

(*Received* 21 *July* 1986; *accepted* 17 *November* 1986)

Abstract

An idealized structure model of the $K_3Nb_7O_{19}$ compound has been deduced from high-resolution electron micrographs. For simplicity the structure was derived in a pseudo-monoclinic system with triclinic symmetry (space group $P\bar{1}$) and unit-cell dimensions $a = 13{\cdot}777\ (2)$, $b = 6{\cdot}431\ (1)$, $c = 18{\cdot}897\ (6)$ Å, $\alpha \simeq 90$, $\beta = 98{\cdot}06\ (2)$ and $\gamma \simeq 90°$, $V = 1657{\cdot}7$ Å^3, $Z = 4$. It has been verified both by simulated image calculations in two projections and by X-ray powder diffraction studies. The structure consists of a three-dimensional framework which is built up of pairs of NbO_6 octahedra having one edge in common in such a way that the structure can be described by means of {011} crystallographic shear in the ReO_3 type structure. The pairs are linked by edge and corner sharing as in the {120} crystallographic-shear (CS) structure M_7O_{20}. Two kinds of tunnels are formed, in which the K atoms are located. The structure thus independently derived agrees with that recently published by Fallon, Gatehouse & Guddat [*J. Solid State Chem.* (1986), **61**, 181-189], which was determined from single-crystal X-ray data, although their unit cell is triclinic. We have refined the cell parameters given in that article: $a = 14{\cdot}1282\ (9)$, $b = 9{\cdot}9369\ (9)$, $c = 6{\cdot}4553\ (6)$ Å, $\alpha = 106{\cdot}44\ (1)$, $\beta = 95{\cdot}856\ (6)$ and $\gamma = 97{\cdot}30\ (1)°$, $V = 853{\cdot}05$ Å^3, $Z = 2$, $M_r = 1071{\cdot}64$, and $D_x = 4{\cdot}17$ g cm^{-3}. However, in this paper the structure is described in a different manner and discussed in relation to neighbouring compounds of this system. The JCPDS Diffraction File No. for $K_3Nb_7O_{19}$ is 38-1499.

Introduction

High-resolution electron microscopy (HREM) studies of some phases occurring in the $KNbO_3$-Nb_2O_5 system have recently been published (Lundberg & Sundberg, 1986). That article is focused on three different types of tetragonal tungsten bronze (TTB) structure and a block structure, $KNb_{13}O_{33}$. In addition to these compounds, there exist two kinds of layer structures, namely $K_4Nb_6O_{17}$ (Gasperin & Le Bihan, 1982) and *L*-KNb_3O_8 (Gasperin, 1982), both determined by single-crystal X-ray diffraction. A survey of the $KNbO_3$-Nb_2O_5 system published by Roth, Parker, Brower & Minor (1974) included

0108-7681/87/030238-07$01.50